

Theory of Magnetoacoustic Resonance to Probe Multipole Effects Due to a Crystal Field Quartet

Mikito Koga¹ and Masashige Matsumoto²

¹*Department of Physics, Faculty of Education, Shizuoka University, Shizuoka 422–8529, Japan*

²*Department of Physics, Faculty of Science, Shizuoka University, Shizuoka 422–8529, Japan*

We present a new method of acoustically driven resonance that probes octupole degrees of freedom as well as a quadrupole usually hidden by the magnetic properties of a crystal field quartet. A characteristic of the quadrupole is reflected in the anisotropic resonance transition rate, which depends on the propagation direction of a surface acoustic wave under an external magnetic field parallel to a typical crystallographic axis. The transition rate is modulated by the anisotropic Zeeman splitting associated with octupoles. We demonstrate how to obtain information about the quartet quadrupole–strain coupling and evaluate the anisotropic octupole effect quantitatively. We also discuss the applicability of our method to identifying a quadrupole order parameter using a multipole–multipole interaction model. For large excitation energy gaps under strong magnetic fields, we propose a photon-assisted magnetoacoustic resonance formulated on the basis of the Floquet theory.

1. Introduction

A crystal field quartet comprises fourfold degenerate electronic states represented by a pseudospin-3/2 operator.^{1,2} Unlike a pure spin, it shows anisotropic Zeeman splitting in the presence of a magnetic field.³ The origin of the anisotropy can be understood as an effect of octupole components produced by the spin-3/2 operators, which are coupled to the magnetic field in the same way as dipole components.

For the spin-3/2 electronic states, the quadrupole degrees of freedom are coupled to strain fields driven by external oscillating perturbations such as surface or bulk acoustic waves.^{4–6} According to room temperature spin-acoustic resonance (SAR) measurements in silicon carbide (4H-SiC),⁷ the electronic ground state of silicon vacancy (V_{Si}) centers can be described by a spin-3/2 quartet, and a characteristic of the quadrupole appears as an anisotropic magnetoacoustic resonance (MAR) transition rate under the rotation of a static magnetic field.⁸ It is also natural that the quartet possesses octupole degrees of freedom.⁹ So far, little attention has been paid to octupoles in the realization of the quantum control of spin-3/2 quartets that will lead to an idea of operating such V_{Si} spins as qubits, namely, four-level systems for quantum information and sensing applications.^{9–15} Indeed, the Zeeman splitting of the V_{Si} quartet shows little magnetic anisotropy under a strong field (~ 10 mT) and behaves like a pure spin-3/2.⁷ This indicates that the octupole effect is quite weak and hardly detected compared with f -electron quartets with relatively strong spin-orbit coupling. A typical example of the crystal field quartet is the Γ_8 representation of the cubic point group O_h . The evidence of octupole effects attributed to a Γ_8 quartet has been reported in numerous studies of Ce-based f -electron systems such as CeB_6 ,^{3,16–25} although it is still highly difficult to directly probe a characteristic of the octupole, which is usually hidden by the Γ_8 magnetic properties, as well as that of the quadrupole.

Motivated by the observation of the field-orientation-dependent SAR,⁷ we presented a more detailed theoretical description of the realistic spin–strain interaction for spin-3/2 to quantitatively evaluate the spin–strain coupling parameters

from the resonance transition rate.⁸ In this paper, we apply our previous theory to the crystal field quartet in a different way. Unlike the isotropic spin-3/2, the energy differences between the quartet sublevels change with the rotation of a magnetic field, so that the readjustment of a resonance condition is inevitably required. To avoid this, we change the propagation direction of a standing surface acoustic wave (SAW) that drives strain fields being coupled to the quartet, where the direction of the magnetic field is fixed at a typical crystallographic axis. For an $O_h \Gamma_8$ quartet, we choose the field parallel to $[110]$ or $[111]$. In actual MAR measurements, it is sufficient to adopt a few propagation directions of SAWs to obtain the information about (1) coupling parameters in the spin–strain (quadrupole–strain) interaction and (2) an octupole effect associated with anisotropic Zeeman splitting of the quartet. Indeed, the quantitative evaluation of these quantities is required for the quantum control of solid-state spin multiplets considering the fine structure.⁹ Thus, the method of MAR proposed here has the great advantage as a microscopic probe of both quadrupole and octupole features possessed by the spin multiplets.

In general, the multipole order phase depends on the direction of a magnetic field. This is attributable to the anisotropic Zeeman splitting, as mentioned above, which can be represented by the octupole components classified into the point group representations. The octupole effect is significant for the Γ_8 multipole–multipole interaction systems having a nearly $SU(4)$ symmetry, such as CeB_6 .³ On the basis of a spherical interaction model, we demonstrate how to identify a quadrupole order parameter depending on the field direction using MAR.

Currently, the frequency of an SAW-induced strain field is limited up to gigahertz order. Usually, a relatively strong magnetic field is required for precise measurements, and a necessary resonance condition for MAR possibly exceeds ten gigahertz order in energy. To realize the MAR in large excitation energy gaps, we propose a possible method combining a microwave with strain fields.^{26–29} The difficulty can be resolved by a high-frequency photon absorption transition using a lin-

early polarized microwave, which is accompanied by a simultaneous low-frequency phonon absorption. The total transition process is analogous with bichromatic driving for electron spin resonance (ESR) measurements.^{30–32} On the basis of the Floquet theory,^{33,34} we formulate the hybrid MAR as a useful method for the evaluation of the quadrupole-coupling strengths associated with the phonon absorption.

This paper is organized as follows. In Sect. 2, we describe the multipole degrees of freedom for a Γ_8 quartet and the anisotropic Zeeman splitting derived from the octupoles under the rotation of a magnetic field. In Sect. 3, we formulate a theory of acoustically driven resonance transition depending on the SAW propagation directions considering the quadrupole–strain interactions under the typical field directions. How to evaluate an octupole effect is explained, and lastly, our proposal for the hybrid MAR measurements is presented. The conclusion of this paper is given in Sect. 4. In Appendix A, we list the multipole operators with the 4×4 matrix form. The equations listed in Appendices B and C are used for the anisotropic Zeeman and quadrupole–strain coupling terms, respectively, under the field rotation. In Appendix D, the multipole operators are represented by pseudospins for spin and orbital degrees of freedom in the quartet. To discuss anisotropic magnetic field dependences arising from the Zeeman splitting in a quadrupole order phase, we introduce a multipole–multipole interaction model in Appendix E, and demonstrate how the octupole effects are derived from the Ginzburg–Landau (GL) expansion of the free energy for the typical field directions in Appendix F.

2. Magnetic Field Effect on a Crystal Field Quartet

2.1 Multipole degrees of freedom

To investigate multipole degrees of freedom in a crystal field quartet, we consider the following $J = 5/2$ Γ_8 states for the cubic point group O_h :

$$\begin{aligned} |\Gamma_{8,1}\rangle &= -\sqrt{\frac{1}{6}}|3/2\rangle - \sqrt{\frac{5}{6}}|-5/2\rangle, \\ |\Gamma_{8,2}\rangle &= |1/2\rangle, \\ |\Gamma_{8,3}\rangle &= -|-1/2\rangle, \\ |\Gamma_{8,4}\rangle &= \sqrt{\frac{5}{6}}|5/2\rangle + \sqrt{\frac{1}{6}}|3/2\rangle, \end{aligned} \quad (1)$$

where $|M\rangle$ ($M = 5/2, 3/2, \dots, -5/2$) represents one of the J_z states with total angular momentum $J = 5/2$. The multipoles of the $J = 5/2$ moment are described by tensor operators, which are expressed by the products of the angular momentum operators $\{J_x, J_y, J_z\}$. Because we here restrict ourselves to multipoles in the Γ_8 quartet, the irreducible tensor operators for the Γ_8 basis can be expressed by effective $J = 3/2$ dipole (rank-1), quadrupole (rank-2), and octupole (rank-3) operators. The irreducible tensor operators $J_q^{(p)}$ of rank p ($q = p, p-1, \dots, -p$) are constructed using the following formula:³⁵

$$J_p^{(p)} = (-1)^p \sqrt{\frac{(2p-1)(2p-3)\cdots 3 \cdot 1}{2p(2p-2)\cdots 2}} J_+^p, \quad (2)$$

$$J_{q-1}^{(p)} = \frac{1}{\sqrt{(p+q)(p-q+1)}} [J_-, J_q^{(p)}], \quad (3)$$

and $J_\pm = J_x \pm iJ_y$. In Appendix A, we list the three dipole, five quadrupole, and seven octupole operators for O_h , and show the corresponding 4×4 matrices for $J = 3/2$.

Let us represent the Γ_8 quartet by $J_{\Gamma_8} = 3/2$ pseudospin as $\{|\Gamma_{8,1}\rangle, |\Gamma_{8,2}\rangle, |\Gamma_{8,3}\rangle, |\Gamma_{8,4}\rangle\} \rightarrow \{|3/2\rangle, |1/2\rangle, |-1/2\rangle, |-3/2\rangle\}$. The matrix expressions of $J_{\Gamma_8} = 3/2$ dipole operators are obtained by calculating the matrix elements of $J = 5/2$ dipole operators in the Γ_8 subspace as

$$\begin{aligned} J_{x,\Gamma_8} &= \begin{pmatrix} 0 & -\frac{1}{\sqrt{3}} & 0 & -\frac{5}{6} \\ -\frac{1}{\sqrt{3}} & 0 & -\frac{3}{2} & 0 \\ 0 & -\frac{3}{2} & 0 & -\frac{1}{\sqrt{3}} \\ -\frac{5}{6} & 0 & -\frac{1}{\sqrt{3}} & 0 \end{pmatrix}, \\ J_{y,\Gamma_8} &= \begin{pmatrix} 0 & \frac{i}{\sqrt{3}} & 0 & -\frac{5}{6} \\ -\frac{i}{\sqrt{3}} & 0 & \frac{3}{2} & 0 \\ 0 & -\frac{3}{2} & 0 & \frac{i}{\sqrt{3}} \\ \frac{5}{6} & 0 & -\frac{i}{\sqrt{3}} & 0 \end{pmatrix}, \\ J_{z,\Gamma_8} &= \begin{pmatrix} -\frac{11}{6} & 0 & 0 & 0 \\ 0 & \frac{1}{2} & 0 & 0 \\ 0 & 0 & -\frac{1}{2} & 0 \\ 0 & 0 & 0 & \frac{11}{6} \end{pmatrix}. \end{aligned} \quad (4)$$

With Eqs. (A.1) and (A.4), the dipole components in Eq. (4) are represented by the linear combination of $J = 3/2$ dipole J_μ and octupole T_μ^α operators: $J_{\mu,\Gamma_8} = -J_\mu - (4/9)T_\mu^\alpha$ ($\mu = x, y, z$). The spin-orbit coupling brings about anisotropic Zeeman splitting described by T_μ^α in J_{μ,Γ_8} . To investigate the octupole effect, we generalize J_{μ,Γ_8} by introducing an anisotropy parameter λ as the coefficient of T_μ^α in the following discussion. For a large λ , the Zeeman splitting strongly depends on the field direction. The Zeeman term is then given by the following Hamiltonian,

$$H_Z = g_J \mu_B \sum_\mu J_{\mu,\Gamma_8} H_\mu = g_J \mu_B \sum_\mu (-J_\mu - \lambda T_\mu^\alpha) H_\mu \quad (\mu = x, y, z), \quad (5)$$

with the external magnetic field $\mathbf{H} = (H_x, H_y, H_z)$. Here, μ_B is the Bohr magneton and g_J is Landé's g factor ($g_J = 6/7$ for localized f -electrons with $J = 5/2$).

2.2 Zeeman splitting under field rotation

The cubic reference frame is defined by the coordinates $\{x, y, z\}$ with the three orthogonal vectors $\mathbf{e}_x = (1, 0, 0)$, $\mathbf{e}_y = (0, 1, 0)$, and $\mathbf{e}_z = (0, 0, 1)$. To describe the Zeeman splitting under the magnetic field \mathbf{H} , it is convenient to use a different reference frame where the field direction is chosen as the quantization axis Z . The polar representation of the field is written as $\mathbf{H} = H e_Z$ with $\mathbf{e}_Z =$

($\sin \theta \cos \phi, \sin \theta \sin \phi, \cos \theta$); the other orthogonal unit vectors are defined as $e_X = (-\cos \theta \cos \phi, -\cos \theta \sin \phi, \sin \theta)$ and $e_Y = (\sin \phi, -\cos \phi, 0)$. In the new (XYZ) reference frame, we define the following unitary transformation: $J_\nu = U^\dagger(e_\nu \cdot \mathbf{J})U$ ($\nu = X, Y, Z$). Here, the operator U is given by the 4×4 matrix form in Appendix B. The dipole term in Eq. (5) is then transformed as

$$U^\dagger \left(\sum_\mu J_\mu B_\mu \right) U = J_Z B \quad (B_\mu \equiv g_J \mu_B H_\mu, B \equiv g_J \mu_B H), \quad (6)$$

while the transformed octupole term becomes very complicated. After a lengthy calculation, we obtain

$$\begin{aligned} U^\dagger \left(\sum_\mu T_\mu^\alpha B_\mu \right) U &= f_1 T_Z^\alpha + f_2 T_Z^\beta + f_3 T_{XYZ} \\ &+ f_4 \left(\sqrt{\frac{3}{8}} T_X^\alpha + \sqrt{\frac{5}{8}} T_X^\beta \right) + f_5 \left(\sqrt{\frac{5}{8}} T_X^\alpha - \sqrt{\frac{3}{8}} T_X^\beta \right) \\ &+ f_6 \left(\sqrt{\frac{3}{8}} T_Y^\alpha - \sqrt{\frac{5}{8}} T_Y^\beta \right) + f_7 \left(-\sqrt{\frac{5}{8}} T_Y^\alpha - \sqrt{\frac{3}{8}} T_Y^\beta \right), \end{aligned} \quad (7)$$

where the coefficients f_i ($i = 1, 2, \dots, 7$) are given in Eq. (B.3). The Zeeman splitting is described by the transformed Hamiltonian

$$\tilde{H}_Z = U^\dagger \sum_\mu (-J_\mu - \lambda T_\mu^\alpha) B_\mu U \quad (8)$$

in the (XYZ) reference frame. Owing to the cubic symmetry, the octupole part is reduced to simpler forms in the specific field directions $\mathbf{H} \parallel [110]$ ($\cos \theta = 0, \sin \theta = 1, \phi = \pi/4$) and $\mathbf{H} \parallel [111]$ ($\cos \theta = \sqrt{1/3}, \sin \theta = \sqrt{2/3}, \phi = \pi/4$). For $\mathbf{H} \parallel [110]$, the explicit matrix form is given by

$$\begin{aligned} \tilde{H}_{Z,[110]} &= B \left[-J_Z - \lambda \left(-\frac{1}{4} T_Z^\alpha - \frac{\sqrt{15}}{4} T_Z^\beta \right) \right] \\ &= -\frac{B}{16} \begin{pmatrix} 24 - 3\lambda & 0 & -15\sqrt{3}\lambda & 0 \\ 0 & 8 + 9\lambda & 0 & 15\sqrt{3}\lambda \\ -15\sqrt{3}\lambda & 0 & -8 - 9\lambda & 0 \\ 0 & 15\sqrt{3}\lambda & 0 & -24 + 3\lambda \end{pmatrix}. \end{aligned} \quad (9)$$

For $\mathbf{H} \parallel [111]$,

$$\begin{aligned} \tilde{H}_{Z,[111]} &= B \left\{ -J_Z - \lambda \left[-\frac{2}{3} T_Z^\alpha + \frac{\sqrt{5}}{3} \left(\sqrt{\frac{5}{8}} T_X^\alpha - \sqrt{\frac{3}{8}} T_X^\beta \right) \right] \right\} \\ &= -\frac{B}{4} \begin{pmatrix} 6 - 2\lambda & 0 & 0 & 5\sqrt{2}\lambda \\ 0 & 2 + 6\lambda & 0 & 0 \\ 0 & 0 & -2 - 6\lambda & 0 \\ 5\sqrt{2}\lambda & 0 & 0 & -6 + 2\lambda \end{pmatrix}. \end{aligned} \quad (10)$$

Diagonalizing these matrices, we obtain the eigenvalues $E_{Z,i}$ ($i = 1, 2, 3, 4$) and the corresponding eigenstates $|\psi_i\rangle$ as listed in Table I.

Table I. Eigenenergies normalized by $B = g_J \mu_B H$ and the corresponding eigenstates of a crystal field quartet split by the magnetic fields $\mathbf{H} \parallel [110]$ and $\mathbf{H} \parallel [111]$. Each eigenstate is described by the $J = 3/2$ states $|M\rangle$ ($M = 3/2, 1/2, -1/2, -3/2$), which are quantized with respect to the field direction. The anisotropic parameter λ represents an octupole effect on the Zeeman splitting.

$E_{Z,i}$ for $\mathbf{H} \parallel [110]$	$ \psi_i\rangle$
$E_{Z,1} = -\frac{1}{8} \left(4 - 3\lambda + \frac{F_\lambda}{2} \right)$	$ \psi_1\rangle = c_+ \frac{3}{2} \rangle + c_- -\frac{1}{2} \rangle$
$E_{Z,2} = -\frac{1}{8} \left(-4 + 3\lambda + \frac{F_\lambda}{2} \right)$	$ \psi_2\rangle = -c_- -\frac{3}{2} \rangle + c_+ \frac{1}{2} \rangle$
$E_{Z,3} = \frac{1}{8} \left(-4 + 3\lambda + \frac{F_\lambda}{2} \right)$	$ \psi_3\rangle = -c_- \frac{3}{2} \rangle + c_+ -\frac{1}{2} \rangle$
$E_{Z,4} = \frac{1}{8} \left(4 - 3\lambda + \frac{F_\lambda}{2} \right)$	$ \psi_4\rangle = c_+ -\frac{3}{2} \rangle + c_- \frac{1}{2} \rangle$
<hr/>	
$F_\lambda = \sqrt{(16 + 3\lambda)^2 + (15\sqrt{3}\lambda)^2}$,	$c_\pm = \pm \sqrt{\frac{1}{2} \left(1 \pm \frac{16 + 3\lambda}{F_\lambda} \right)}$

$E_{Z,i}$ for $\mathbf{H} \parallel [111]$	$ \psi_i\rangle$
$E_{Z,1} = -\frac{1}{4} G_\lambda$	$ \psi_1\rangle = d_+ \frac{3}{2} \rangle + d_- -\frac{3}{2} \rangle$
$E_{Z,2} = -\frac{1}{2} (1 + 3\lambda)$	$ \psi_2\rangle = \frac{1}{2} \rangle$
$E_{Z,3} = \frac{1}{2} (1 + 3\lambda)$	$ \psi_3\rangle = -\frac{1}{2} \rangle$
$E_{Z,4} = \frac{1}{4} G_\lambda$	$ \psi_4\rangle = -d_- \frac{3}{2} \rangle + d_+ -\frac{3}{2} \rangle$
<hr/>	
$G_\lambda = \sqrt{(6 - 2\lambda)^2 + 50\lambda^2}$,	$d_\pm = \sqrt{\frac{1}{2} \left(1 \pm \frac{6 - 2\lambda}{G_\lambda} \right)}$

3. Acoustically Driven Resonance Transition

3.1 Quadrupole–strain interaction under the field rotation

In the local O_h systems, the quadrupole–strain interaction is described by the following Hamiltonian:³⁶⁾

$$H_\varepsilon = g_3 (O_u \varepsilon_u + O_v \varepsilon_v) + g_5 (O_{zx} \varepsilon_{zx} + O_{xy} \varepsilon_{xy} + O_{yz} \varepsilon_{yz}), \quad (11)$$

with the two independent coupling constants g_3 and g_5 . Each quadrupole is coupled to the corresponding strain tensor $\varepsilon_{\mu\nu}$ ($\mu, \nu = x, y, z$) and

$$\varepsilon_u \equiv \frac{1}{\sqrt{3}} (2\varepsilon_{zz} - \varepsilon_{xx} - \varepsilon_{yy}), \quad \varepsilon_v \equiv \varepsilon_{xx} - \varepsilon_{yy}. \quad (12)$$

For the magnetic field $\mathbf{H} \parallel Z$, we apply the unitary transformation to H_ε using Eq. (B.1) and obtain its form in the (XYZ) reference frame as⁸⁾

$$\tilde{H}_\varepsilon = U^\dagger H_\varepsilon U = \sum_K A_K O_K, \quad (13)$$

where O_K ($K = U, V, ZX, XY, YZ$) are the quadrupole operators in the (XYZ) reference frame. As shown in Appendix C, each unitary transformed O_k is given by the linear combination of the five components O_K . Accordingly, the strain-dependent coupling coefficients A_K depend on the field direction represented by θ and ϕ .

3.2 Single-phonon transition rate depending on propagation directions of SAW

We consider that the local quartet is coupled to the strain fields driven by a plane Rayleigh SAW propagating on the xy plane, as shown in Fig. 1. The strain tensors are described by

$$\varepsilon_{\alpha\beta}(t, x', z) = \varepsilon_{\alpha\beta}(z) e^{ikx' - i\omega t} + \varepsilon_{\alpha\beta}^*(z) e^{-ikx' + i\omega t}, \quad (14)$$

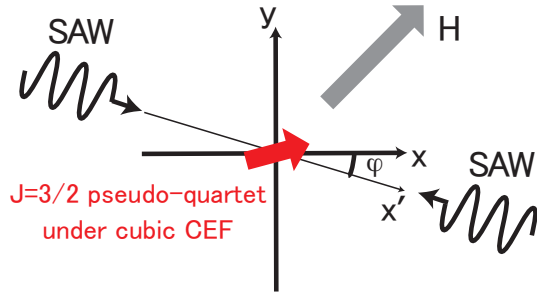


Fig. 1. (Color online) Illustration of pseudo-quartet represented by $J = 3/2$ operator in a cubic crystalline electric field (CEF) environment, which is coupled to SAWs propagating in the $\pm x'$ directions under the static magnetic field \mathbf{H} . The angle φ of the x' -axis is measured from the crystallographic x -axis.

where the x' -axis denotes the direction of the propagating SAW, nonzero components $\alpha\beta$ are restricted to $\{x'x', zz, x'z\}$ (no displacement along y'), and the amplitudes of strain tensors only depend on the depth z from the surface layer (xy plane). We assume that $\varepsilon_{x'x'}$ and ε_{zz} are real, whereas $\varepsilon_{x'z} \equiv -i\varepsilon''_{x'z}$ is purely imaginary ($\varepsilon''_{x'z}$ is real).⁷⁾ This indicates an elliptical polarization of the SAW medium. When the x' -axis is rotated from x by angle φ in the xy plane, the coordinates are transformed as⁸⁾

$$\begin{pmatrix} x' \\ y' \end{pmatrix} = \begin{pmatrix} \cos \varphi & \sin \varphi \\ -\sin \varphi & \cos \varphi \end{pmatrix} \begin{pmatrix} x \\ y \end{pmatrix}, \quad (15)$$

and the strain tensor components in Eq. (C-2) are replaced as

$$\begin{aligned} \varepsilon_{xx} &\rightarrow \varepsilon_{x'x'} \cos^2 \varphi, & \varepsilon_{yy} &\rightarrow \varepsilon_{x'x'} \sin^2 \varphi, & \varepsilon_{xy} &\rightarrow \varepsilon_{x'x'} \sin \varphi \cos \varphi, \\ \varepsilon_{zx} &\rightarrow \varepsilon_{x'z} \cos \varphi, & \varepsilon_{yz} &\rightarrow \varepsilon_{x'z} \sin \varphi. \end{aligned} \quad (16)$$

Here, $\varepsilon_{\alpha\beta} = 0$ when either α or β is y' .

From now on, we restrict ourselves to the two cases of field direction in Table I to calculate the transition matrix element between two quartet states $M_{mn,\pm} = \langle \psi_m | \hat{H}_\varepsilon | \psi_n \rangle$ using Eq. (13), where the transition is caused by the absorption of a single phonon. The subscripts $+$ and $-$ denote $+x'$ and $-x'$ propagation directions of the SAW, respectively. For the latter, k is replaced by $-k$ in Eq. (14), and $\varepsilon''_{x'z} \rightarrow -\varepsilon''_{x'z}$ is required. For $\mathbf{H} \parallel [110]$, we obtain the transition matrix elements associated with the ground state $|\psi_1\rangle$:

$$\begin{aligned} M_{21,+} &= i\sqrt{3} \left[g_3 \varepsilon_{x'x'} \cos 2\varphi - g_5 \varepsilon''_{x'z} \cos \left(\varphi - \frac{\pi}{4} \right) \right], \\ M_{31,+} &= \left[c_+ c_- + \frac{\sqrt{3}}{2} (c_+^2 - c_-^2) \right] g_3 (2\varepsilon_{zz} - \varepsilon_{x'x'}) \\ &\quad + \left[-\frac{3}{2} c_+ c_- + \frac{\sqrt{3}}{4} (c_+^2 - c_-^2) \right] g_5 \varepsilon_{x'x'} \sin 2\varphi \\ &\quad + \sqrt{3} g_5 \varepsilon''_{x'z} \cos \left(\varphi + \frac{\pi}{4} \right), \\ M_{41,+} &= 0, \end{aligned} \quad (17)$$

and $M_{mn,+} = M_{nm,+}^*$. In the same manner, for $\mathbf{H} \parallel [111]$,

$$\begin{aligned} M_{21,+} &= \left(\sqrt{\frac{2}{3}} d_+ + \frac{d_-}{\sqrt{3}} \right) g_3 (2\varepsilon_{zz} - \varepsilon_{x'x'}) \\ &\quad + i \left(\sqrt{2} d_+ + d_- \right) g_3 \varepsilon_{x'x'} \cos 2\varphi \end{aligned}$$

$$\begin{aligned} &+ \left(-\frac{d_+}{\sqrt{6}} + \frac{d_-}{\sqrt{3}} \right) g_5 \varepsilon_{x'x'} \sin 2\varphi \\ &+ (d_+ - \sqrt{2} d_-) g_5 \varepsilon''_{x'z} \cos \left(\varphi + \frac{\pi}{4} \right) \\ &+ i \left(-\frac{d_+}{\sqrt{3}} + \sqrt{\frac{2}{3}} d_- \right) g_5 \varepsilon''_{x'z} \cos \left(\varphi - \frac{\pi}{4} \right), \\ M_{31,+} &= \left(-\sqrt{\frac{2}{3}} d_- + \frac{d_+}{\sqrt{3}} \right) g_3 (2\varepsilon_{zz} - \varepsilon_{x'x'}) \\ &+ i \left(\sqrt{2} d_- - d_+ \right) g_3 \varepsilon_{x'x'} \cos 2\varphi \\ &+ \left(\frac{d_-}{\sqrt{6}} + \frac{d_+}{\sqrt{3}} \right) g_5 \varepsilon_{x'x'} \sin 2\varphi \\ &+ (d_- + \sqrt{2} d_+) g_5 \varepsilon''_{x'z} \cos \left(\varphi + \frac{\pi}{4} \right) \\ &+ i \left(\frac{d_-}{\sqrt{3}} + \sqrt{\frac{2}{3}} d_+ \right) g_5 \varepsilon''_{x'z} \cos \left(\varphi - \frac{\pi}{4} \right), \\ M_{41,+} &= 0. \end{aligned} \quad (18)$$

Now, we are prepared to calculate the single-phonon transition rate W_{n1} between the ground and n th excited states of the quartet. We here consider the case of a standing SAW where the quartet is coupled simultaneously to two SAWs propagating along the $+x'$ and $-x'$ directions with equal intensities. Indeed, a standing wave was realized in a recent spin acoustic resonance experiment.⁷⁾ Thus, the rate W_{n1} is proportional to the sum of the $\pm x'$ propagating SAW contributions,

$$W_{n1} \propto \frac{1}{2} (|M_{n1,+}|^2 + |M_{n1,-}|^2), \quad (19)$$

where the bracket $\langle \dots \rangle$ indicates averaging the strain amplitudes with respect to the spatial distributions of magnetic ions with the quartets. We have also assumed that the coherence terms such as $\langle \text{Re}[M_{n1,+}^* M_{n1,-}] \cdot \cos 2kx' \rangle$ are canceled out by the average over the ion positions.

Under the magnetic field \mathbf{H} , the rate W_{n1}^H is calculated as a function of φ :

$$W_{n1}^H(\varphi) \propto A_{n1}^H + B_{n1}^H \sin 2\varphi + C_{n1}^H \cos 4\varphi. \quad (20)$$

For $\mathbf{H} \parallel [110]$, the coefficients in W_{21}^H are given by

$$\begin{aligned} A_{21}^{[110]} &= \frac{1}{2} (g_3^2 \langle \varepsilon_{x'x'}^2 \rangle + g_5^2 \langle \varepsilon_{x'z}^{\prime 2} \rangle), \\ B_{21}^{[110]} &= \frac{1}{2} g_5^2 \langle \varepsilon_{x'z}^{\prime 2} \rangle, \\ C_{21}^{[110]} &= \frac{1}{2} g_3^2 \langle \varepsilon_{x'x'}^2 \rangle. \end{aligned} \quad (21)$$

Here, $\langle \dots \rangle$ represents an average over the z direction. In Fig. 2(a), the polar representation of $W_{21}(\varphi)$ is plotted for various values of the ratio $g_5^2 \langle \varepsilon_{x'z}^{\prime 2} \rangle / g_3^2 \langle \varepsilon_{x'x'}^2 \rangle$. As the ratio increases, the term $\sin 2\varphi$ becomes more dominant than $\cos 4\varphi$, and the latter is characterized by a V-shaped feature at $\varphi = \pi/4$ that matches the field direction. Similarly, for the rate $W_{31}^{[110]}$,

$$\begin{aligned} A_{31}^{[110]} &= (\alpha_3 g_3)^2 \langle (2\varepsilon_{zz} - \varepsilon_{x'x'})^2 \rangle + \frac{1}{2} g_5^2 (\alpha_5^2 \langle \varepsilon_{x'x'}^2 \rangle + \langle \varepsilon_{x'z}^{\prime 2} \rangle), \\ B_{31}^{[110]} &= 2\alpha_3 \alpha_5 g_3 g_5 \langle (2\varepsilon_{zz} - \varepsilon_{x'x'}) \varepsilon_{x'x'} \rangle - \frac{1}{2} g_5^2 \langle \varepsilon_{x'z}^{\prime 2} \rangle, \end{aligned}$$

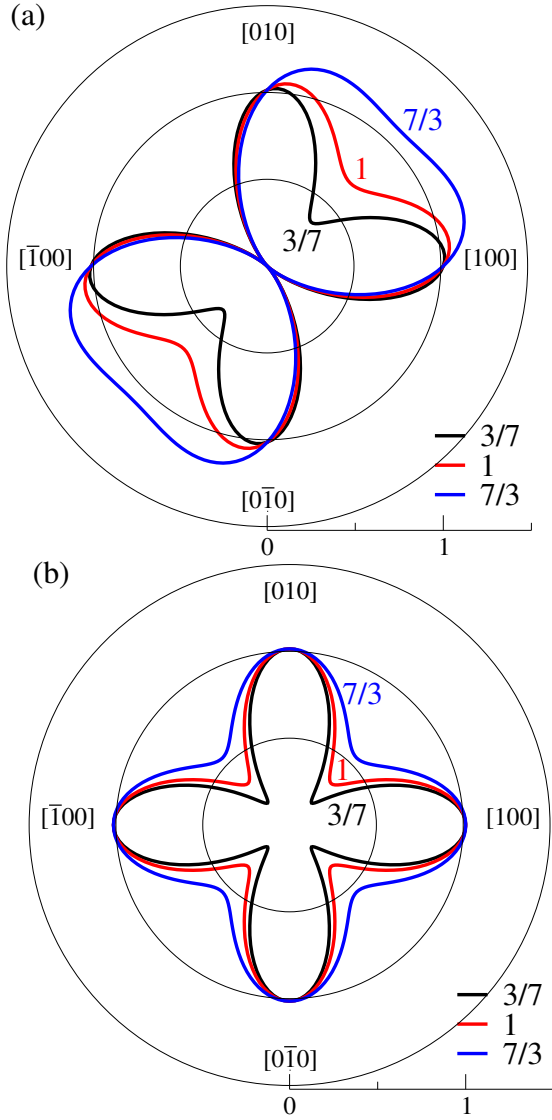


Fig. 2. (Color online) Polar representation of transition rate for $\mathbf{H} \parallel [110]$ with respect to the angle φ of the SAW propagation direction in Eq. (20). The data plotted here are normalized by the values at $\varphi = 0$. (a) Plotting of $W_{21}^{[110]}(\varphi)$ for $g_5^2 \langle \varepsilon_{x'z}^2 \rangle / g_3^2 \langle \varepsilon_{x'x'}^2 \rangle = 3/7$ (black), 1 (red), and $7/3$ (blue). (b) $W_{21}^{[110]}(\varphi) + W_{21}^{[110]}(-\varphi)$ for evaluating the amplitude $C_{21}^{[110]}$ of the $\cos 4\varphi$ term.

$$C_{31}^{[110]} = -\frac{1}{2}(\alpha_5 g_5)^2 \langle \varepsilon_{x'x'}^2 \rangle, \quad (22)$$

where

$$\alpha_3 = \frac{c_+ c_-}{\sqrt{3}} + \frac{c_+^2 - c_-^2}{2}, \quad \alpha_5 = -\frac{\sqrt{3}}{2} c_+ c_- + \frac{c_+^2 - c_-^2}{4}. \quad (23)$$

In particular, we focus on C_{n1}^H in the term of $\cos 4\varphi$ to evaluate the ratio of coupling constants $r_g \equiv g_5/g_3$ in Eq. (11) because it contains only $\langle \varepsilon_{x'x'}^2 \rangle$ among various strain components. For this purpose, the contribution from the term of $\cos 4\varphi$ is extracted by plotting $W_{n1}^H(\varphi) + W_{n1}^H(-\varphi)$, as shown in Fig. 2(b). Indeed, the value of C_{n1}^H can be obtained from measurable values of W_{n1}^H as

$$C_{n1}^H \propto 2W_{n1}^H(0) - W_{n1}^H(\pi/4) - W_{n1}^H(-\pi/4). \quad (24)$$

From Table I, α_5 is given as a function of λ representing the

octupole contribution, which leads to

$$-\frac{C_{31}^{[110]}}{C_{21}^{[110]}} = \alpha_5^2 r_g^2 = \left(\frac{g_5}{g_3}\right)^2 \frac{16(1+3\lambda)^2}{(16+3\lambda)^2 + (15\sqrt{3}\lambda)^2}. \quad (25)$$

A similar argument can be applied to $W_{n1}^{[111]}$ for $\mathbf{H} \parallel [111]$. Because $C_{n1}^{[111]}$ ($n = 2, 3$) contains the only parameter $\langle \varepsilon_{x'x'}^2 \rangle$ for strain as $C_{21}^{[110]}$ in Eq. (21), we obtain

$$\begin{aligned} \frac{C_{21}^{[111]}}{C_{21}^{[110]}} &= \frac{1}{3} \left[(\sqrt{2}d_+ + d_-)^2 - \frac{r_g^2}{6} (d_+ - \sqrt{2}d_-)^2 \right] \\ &= \left(\frac{1}{2} + \frac{1+3\lambda}{G_\lambda} \right) - \frac{r_g^2}{6} \left(\frac{1}{2} - \frac{1+3\lambda}{G_\lambda} \right), \\ \frac{C_{31}^{[111]}}{C_{21}^{[110]}} &= \frac{1}{3} \left[(d_+ - \sqrt{2}d_-)^2 - \frac{r_g^2}{6} (\sqrt{2}d_+ + d_-)^2 \right] \\ &= \left(\frac{1}{2} - \frac{1+3\lambda}{G_\lambda} \right) - \frac{r_g^2}{6} \left(\frac{1}{2} + \frac{1+3\lambda}{G_\lambda} \right), \end{aligned} \quad (26)$$

where G_λ is given as a function of λ in Table I. Combining these equations, we can evaluate the coupling-constant ratio as

$$\left(\frac{g_5}{g_3}\right)^2 = 6 \left(1 - \frac{C_{21}^{[111]} + C_{31}^{[111]}}{C_{21}^{[110]}} \right). \quad (27)$$

Suppose the parameter λ is unknown, it can also be evaluated using C_{n1}^H as

$$\frac{G_\lambda + 2(1+3\lambda)}{G_\lambda - 2(1+3\lambda)} = \frac{C_{31}^{[111]} - C_{21}^{[110]}}{C_{21}^{[111]} - C_{21}^{[110]}}. \quad (28)$$

For the $J = 5/2 \Gamma_8$ quartet ($\lambda = 4/9$), the calculated value of this ratio equals eight, which is four times larger than that for the pure $J = 3/2$ quartet ($\lambda = 0$).

3.3 Anisotropy of Zeeman effect on quadrupole order phase

It is highly useful to study the octupole effect in the antiferroquadrupole order phase on the basis of the multipole–multipole interaction model given in Appendix E, where we use pseudospin representations for the multipole operators, as introduced in Appendix D. The detailed group theoretical study was first presented by Shiina *et al.*,³⁾ and an important role of octupole degrees of freedom in CeB₆ was elucidated. The spherical interaction Hamiltonian comprises the nonmagnetic part H_Q with a coupling constant D_Q in Eq. (E.4) and the magnetic part H_M with D_M in Eq. (E.5). Note that the forms of both H_Q and H_M are invariant in arbitrary directions of the magnetic field \mathbf{H} . This also holds for $D_Q \neq D_M$ in the combined Hamiltonian of H_Q and H_M , where the symmetry of the interaction is lowered from the SU(4) symmetry satisfying $D_Q = D_M$ in Eq. (E.1). Thus, under the rotation of \mathbf{H} , the model Hamiltonian $\tilde{H}_s = \tilde{H}_Q + \tilde{H}_M + \tilde{H}_Z$ in the (XYZ) reference frame can be written as

$$\tilde{H}_Q = D_Q \sum_{(i,j)} [(\tilde{\tau}_i^Z \tilde{\tau}_j^Z + \tilde{\tau}_i^X \tilde{\tau}_j^X) + (\tilde{\tau}_i^Y \tilde{\sigma}_i) \cdot (\tilde{\tau}_j^Y \tilde{\sigma}_j)], \quad (29)$$

$$\begin{aligned} \tilde{H}_M = D_M \sum_{(i,j)} &[\tilde{\sigma}_i \cdot \tilde{\sigma}_j + (\tilde{\tau}_i^Z \tilde{\sigma}_i) \cdot (\tilde{\tau}_j^Z \tilde{\sigma}_j) \\ &+ (\tilde{\tau}_i^X \tilde{\sigma}_i) \cdot (\tilde{\tau}_j^X \tilde{\sigma}_j) + \tilde{\tau}_i^Y \tilde{\tau}_j^Y], \end{aligned} \quad (30)$$

where the pseudospin representations $\tilde{\sigma} = (\tilde{\sigma}^X, \tilde{\sigma}^Y, \tilde{\sigma}^Z) = 2\sigma$ and $\tilde{\tau} = (\tilde{\tau}^X, \tilde{\tau}^Y, \tilde{\tau}^Z) = 2\tau$ are defined in Appendices D and E. For \tilde{H}_Z in the three typical field directions,

$$\tilde{H}_Z = \begin{cases} B \sum_i \left[\frac{1+3\lambda}{2} \tilde{\sigma}_i^Z + \frac{4-3\lambda}{4} \tilde{\eta}_i^Z \right] & (\mathbf{H} \parallel [001] \parallel Z), \\ B \sum_i \left[\frac{1-2\lambda}{2} \tilde{\sigma}_i^Z + \frac{2+\lambda}{2} \tilde{\eta}_i^Z + \frac{5\lambda}{4\sqrt{2}} (\tilde{\sigma}_i^X + \tilde{\eta}_i^X) \right] & (\mathbf{H} \parallel [111] \parallel Z), \\ B \sum_i \frac{1}{16} [(8-6\lambda)\tilde{\sigma}_i^Z + (16+3\lambda)\tilde{\eta}_i^Z - 15\sqrt{3}\lambda\tilde{\zeta}_i^Z] & (\mathbf{H} \parallel [110] \parallel Z). \end{cases} \quad (31)$$

Here, $\tilde{\eta}^Z = \tilde{\tau}^Z \tilde{\sigma}^Z$, $\tilde{\eta}^X = \tilde{\tau}^Z \tilde{\sigma}^X$, and $\tilde{\zeta}^Z = \tilde{\tau}^X \tilde{\sigma}^Z$ are new representations introduced to the octupole operators. Note that $\tilde{\sigma}^X + \tilde{\eta}^X$ and $\tilde{\zeta}^Z$ have off-diagonal matrix elements of \tilde{H}_Z , as shown in Eqs. (9) and (10).

The primary order parameter is of the quadrupole type for $D_Q > D_M$. According to the mean-field theory,³⁾ the low-field phase is represented by the quadrupole component O_u for $\mathbf{H} \parallel [001]$, $O_{yz} + O_{zx} + O_{xy}$ for $\mathbf{H} \parallel [111]$, and the mixed O_u and O_{xy} for $\mathbf{H} \parallel [110]$. In the (XYZ) reference frame, all three quadrupole components have only diagonal matrix elements of \tilde{H}_Z . The resonance transition rate in Eq. (20) is not affected by the quadrupole order; the only change is a resonance energy shift. The octupole effect causes the increase in the transition temperature T_Q with increasing H , which can be derived from the GL expansion of the free energy in Appendix F.

3.4 Effect of a staggered moment of antiferroquadrupole order on resonance transition rate

For the high-field phase in the highly symmetric interaction model for $D_Q = D_M$, a stable quadrupole component is different from that of the low-field phase.³⁾ One example is the quadrupole order for $\mathbf{H} \parallel [110]$ associated with $O_{yz} + O_{zx}$ that has off-diagonal matrix elements within the two lowest-lying states. When this component is stabilized against the mixed $O_u \oplus O_{xy}$ component in the low H , as mentioned in Sect. 3.3, it is necessary that the Γ_5 -type (O_{yz}, O_{zx}, O_{xy}) intersite quadrupole–quadrupole coupling is slightly larger than the Γ_3 type (O_u and O_v). Indeed, the linear combination of the Γ_5 -type components is considered a prime candidate for the quadrupole order parameter realized in CeB_6 .^{3, 16, 17, 24, 25)} In the (XYZ) reference frame, $O_{yz} + O_{zx}$ corresponds to O_{ZX} related to the pseudospin representation: $2\tau^Y \sigma^Y = O_{ZX}/(2\sqrt{3})$. For $\mathbf{H} \parallel [110]$ in Table I, O_{ZX} has only matrix elements between one pair of $|\psi_1\rangle$ and $|\psi_2\rangle$ and between another pair of $|\psi_3\rangle$ and $|\psi_4\rangle$. In the mean field theory, we consider a staggered moment μ_{af} for the quadrupole component $2\tau^Y \sigma^Y$ in the local Hamiltonian

$$H_{\text{local}}^{(\pm)} = -B \begin{pmatrix} |E_1| & \pm\bar{\mu} \\ \pm\bar{\mu} & |E_2| \end{pmatrix} \left(\bar{\mu} \equiv \frac{D_Q}{B} \mu_{af} \right), \quad (32)$$

for the lowest-lying states $|\psi_1\rangle$ and $|\psi_2\rangle$. Here, the signs \pm of $\bar{\mu}$ are chosen for the two sublattice sites. By diagonalizing $H_{\text{local}}^{(\pm)}$, the eigenenergies and eigenfunctions are obtained as

$$\frac{E_g}{B} = -\frac{F_\lambda}{16} - \bar{E}_\mu \quad |\psi_g\rangle = \cos \theta_\mu |\psi_1\rangle \pm \sin \theta_\mu |\psi_2\rangle,$$

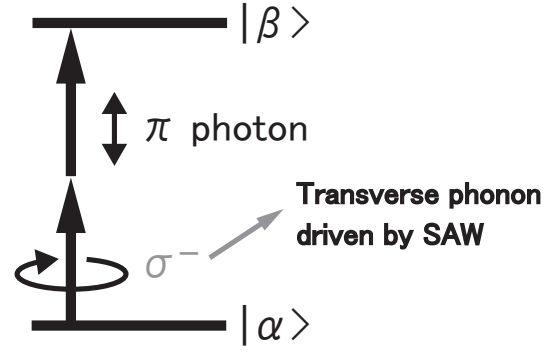


Fig. 3. Analogy of photon-assisted single-phonon transition with the two-photon transition in which left-hand circularly polarized (σ^-) and linearly polarized (π) photons are absorbed between the two electronic states $|\alpha\rangle$ and $|\beta\rangle$. The transverse phonon behaves like the σ^- photon here. The phonon (photon) absorption transition is of a nonmagnetic quadrupole (magnetic dipole) type.

$$\frac{E_e}{B} = -\frac{F_\lambda}{16} + \bar{E}_\mu \quad |\psi_e\rangle = \mp \sin \theta_\mu |\psi_1\rangle + \cos \theta_\mu |\psi_2\rangle, \quad (33)$$

for the ground and first excited states, respectively, where

$$\bar{E}_\mu = \sqrt{\left(\frac{4-3\lambda}{8}\right)^2 + \bar{\mu}^2}, \quad \bar{E}_\mu \cos 2\theta_\mu = \frac{4-3\lambda}{8}, \quad \bar{E}_\mu \sin 2\theta_\mu = \bar{\mu}. \quad (34)$$

As shown in Sect. 3.2, we can calculate the rate $W_{e,g}^{[110]}(\varphi)$ of the acoustically driven resonance transition between $|\psi_g\rangle$ and $|\psi_e\rangle$, and it has the same form as Eq. (20). The effect of the staggered moment μ_{af} can be evaluated on the basis of the deviations from the values of $A_{21}^{[110]}$, $B_{21}^{[110]}$, and $C_{21}^{[110]}$ for $\mu_{af} = 0$ in Eq. (21). In particular, the amplitude $C_{e,g}^{[110]}$ of the $\cos 4\varphi$ term in $W_{e,g}^{[110]}$ is given by the simplest form

$$\frac{C_{e,g}^{[110]}}{C_{21}^{[110]}} = 1 + \frac{6(4-3\lambda)^2}{F_\lambda^2} \frac{g_5^2}{g_3^2} \sin^2 2\theta_\mu. \quad (35)$$

For $\bar{\mu} \approx 0$, it is reduced to

$$\frac{C_{e,g}^{[110]}}{C_{21}^{[110]}} = 1 + \frac{3}{2} \frac{1}{\left(1 + \frac{3\lambda}{16}\right)^2 + \left(\frac{15\sqrt{3}\lambda}{16}\right)^2} \left(\frac{g_5}{g_3}\right)^2 \bar{\mu}^2. \quad (36)$$

This indicates that the amplitude of the $\cos 4\varphi$ term in Eq. (20) for the two lowest-lying levels is increased by the induced quadrupole moment μ_{af} in the $O_{yz} + O_{zx}$ phase for $\mathbf{H} \parallel [110]$. Note that the transition rates between the Γ_8 ground and other excited states are not changed for $\mathbf{H} \parallel [110]$.

3.5 Photon-assisted single-phonon resonance transition

In comparison with the conventional ESR resonance, there are some limitations for increasing the frequency of a strain field induced by SAW of gigahertz order. Usually, an oscillating field of more than ten gigahertz is required to realize the spin resonance transition in the presence of a strong magnetic field. Indeed, this is also the case for CeB_6 where $B \sim 1$ T (order of frequency is ten gigahertz) is the typical energy scale for the resonance condition.

A possible way of achieving acoustically driven spin resonance is to combine a strain field for the transverse coupling with a linearly polarized microwave for the longitudi-

After diagonalizing \tilde{H}_F , we obtain the eigenvalues

$$q_{\pm} = -\frac{n\omega}{2} \pm \tilde{q}_n, \quad (51)$$

where

$$\tilde{q}_n = \sqrt{\frac{(n\omega - \varepsilon_{0A} + 2\delta_n)^2}{4} + |v_{-n}|^2}. \quad (52)$$

Equation (52) leads to the n π -photon time-averaged transition probability from $|\alpha\rangle$ to $|\beta\rangle$,³⁴⁾

$$\bar{P}_{\alpha\rightarrow\beta}^{(n)} = \frac{1}{2} \cdot \frac{|v_{-n}|^2}{\frac{(n\omega - \varepsilon_{0A} + 2\delta_n)^2}{4} + |v_{-n}|^2}. \quad (53)$$

For the single π photon absorption,

$$\bar{P}_{\alpha\rightarrow\beta}^{(1)} = \frac{1}{2} \frac{|A_T J_1|^2}{|A_T J_1|^2 + (\omega - \varepsilon_{0A} + 2\delta_1)^2}. \quad (54)$$

Here, $J_{-1}(x) = -J_1(x)$ is used and $J_1(\Delta/\omega)$ is denoted by J_1 . For the weak coupling limit ($|A_T|, \Delta \ll \omega$), δ_1 and J_1 are approximated as

$$\delta_1 \simeq -\frac{|A_T|^2}{4\varepsilon_{0A}}, \quad J_1 \simeq \frac{\Delta}{2\omega}. \quad (55)$$

Except for $A_T = 0$, the transition probability at $\omega = \varepsilon_{0A}$ is obtained as

$$\bar{P}_{\alpha\rightarrow\beta}^{(1)} = \frac{1}{2} \frac{1}{1 + (|A_T|/\Delta)^2} \quad (\varepsilon_0 = \omega + \omega_A). \quad (56)$$

As given by Eq. (39), the φ dependence of $|A_T|^2$ can be evaluated from the transition probabilities at $\varepsilon_0 = \omega + \omega_A$ measured for various propagation directions of SAW. Even for large excitation energy gaps ε_0 under strong magnetic fields, the MAR is available with the help of optical absorption. The detailed description of this method is beyond the scope of this study.

4. Conclusion

Motivated by the recent progress in acoustic measurements using SAWs, we presented a new idea of MAR to probe multipole degrees of freedom in a crystal field quartet such as an O_h Γ_8 representation. In particular, we focused on an octupole effect on the Zeeman splitting of the quartet, which was explicitly expressed by the anisotropy parameter λ here. We demonstrated how to evaluate λ as well as the ratio of the quadrupole–strain coupling strengths g_5/g_3 from the dependence of the resonance transition rate on the SAW propagation direction represented by φ . The amplitude of the $\cos 4\varphi$ term is a key in the quantitative evaluation. It also provides useful information about the identification of a primary order parameter for multipole–multipole interaction systems. As a simple case, we demonstrated how to confirm an induced Γ_5 -type quadrupole-ordered moment by measuring the amplitude of the $\cos 4\varphi$ term in the MAR. Finally, we proposed a method of photon-assisted single-phonon resonance formulated on the basis of the Floquet theory. This method of using a π photon field is particularly useful for the detection of the acoustically driven phonon transition for rather large excitation energy gaps under strong magnetic fields.

The significant role of octupole degrees of freedom has been studied extensively for the antiferroquadrupole order phase II in CeB₆. In particular, the nuclear magnetic resonance line splitting measured at the B sites was success-

fully explained by considering not only dipole but also octupole moments of a Γ_8 ground state induced by a magnetic field in the quadrupole order phase.^{16,17,37)} The direct evidence of field-induced octupoles was provided by resonant X-ray diffraction measurements²⁴⁾ and inelastic neutron scattering under the rotation of the field direction.²⁵⁾ On the other hand, some open questions about the local Γ_8 scenario have been raised by the observation of ESR signals in a high-field phase^{38–40)} and the recent experiments using B-site nuclear quadrupole resonance in a very low field.⁴¹⁾ So far, no acoustic measurement has been carried out as a microscopic probe of the multipoles. The MAR proposed here can provide direct evidence of whether the local Γ_8 quartet is the origin of the observed multipole features. For the photon-assisted MAR in CeB₆, the frequency of the typical energy scale (10–100 GHz) is accessible by conventional methods using microwaves.

As mentioned in Sect. 1, the V_{Si} quartet is a good candidate for the investigation of the fine structure of the spin-3/2 multipole origin.^{9,42,43)} In particular, a characteristic of the spin quadrupole was actually detected as anisotropic acoustically driven spin resonances at room temperature.⁷⁾ The V_{Si} quartet in SiC has the C_{3v} site symmetry, which makes the V_{Si} spin–strain interaction model more complicated owing to the symmetry lowering from O_h .^{8,44,45)} The dipole and octupole coupling strengths of the Zeeman terms (anisotropic g -factors) are different between the two components parallel to and orthogonal to a typical crystallographic axis.^{42,43)} By considering a complete set of anisotropies associated with the crystal field symmetry, we will develop our method of MAR to reveal a characteristic of the octupole hidden in various defect multiplets.

Acknowledgment This work was supported by JSPS KAKENHI Grant Number 21K03466.

Appendix A: Multipole operators for $J = 3/2$

Here, the irreducible tensor operator representations are listed for the dipole $\{J_x, J_y, J_z\}$, quadrupole $\{O_u, O_v, O_{zx}, O_{xy}, O_{yz}\}$, and octupole $\{T_x^\alpha, T_y^\alpha, T_z^\alpha, T_x^\beta, T_y^\beta, T_z^\beta, T_{xyz}\}$ in the O_h point group.³⁾ The corresponding 4×4 matrices are also presented as follows. For the Γ_4 dipole components,

$$\begin{aligned} J_x &= \frac{1}{\sqrt{2}}(-J_1^{(1)} + J_{-1}^{(1)}) \\ &= \frac{1}{2} \begin{pmatrix} 0 & \sqrt{3} & 0 & 0 \\ \sqrt{3} & 0 & 2 & 0 \\ 0 & 2 & 0 & \sqrt{3} \\ 0 & 0 & \sqrt{3} & 0 \end{pmatrix}, \\ J_y &= \frac{i}{\sqrt{2}}(J_1^{(1)} + J_{-1}^{(1)}) \\ &= \frac{1}{2} \begin{pmatrix} 0 & -i\sqrt{3} & 0 & 0 \\ i\sqrt{3} & 0 & -i2 & 0 \\ 0 & i2 & 0 & -i\sqrt{3} \\ 0 & 0 & i\sqrt{3} & 0 \end{pmatrix}, \\ J_z &= J_0^{(1)} \end{aligned}$$

$$= \frac{1}{2} \begin{pmatrix} 3 & 0 & 0 & 0 \\ 0 & 1 & 0 & 0 \\ 0 & 0 & -1 & 0 \\ 0 & 0 & 0 & -3 \end{pmatrix}. \quad (\text{A.1})$$

For the Γ_3 and Γ_5 quadrupole components,

$$\begin{aligned} O_u &= \frac{1}{\sqrt{3}}(2J_z^2 - J_x^2 - J_y^2) = \frac{2}{\sqrt{3}}J_0^{(2)} \\ &= \sqrt{3} \begin{pmatrix} 1 & 0 & 0 & 0 \\ 0 & -1 & 0 & 0 \\ 0 & 0 & -1 & 0 \\ 0 & 0 & 0 & 1 \end{pmatrix}, \\ O_v &= J_x^2 - J_y^2 = \sqrt{\frac{2}{3}}(J_2^{(2)} + J_{-2}^{(2)}) \\ &= \sqrt{3} \begin{pmatrix} 0 & 0 & 1 & 0 \\ 0 & 0 & 0 & 1 \\ 1 & 0 & 0 & 0 \\ 0 & 1 & 0 & 0 \end{pmatrix}, \end{aligned} \quad (\text{A.2})$$

and

$$\begin{aligned} O_{zx} &= J_x J_x + J_x J_z = \sqrt{\frac{2}{3}}(-J_1^{(2)} + J_{-1}^{(2)}) \\ &= \sqrt{3} \begin{pmatrix} 0 & 1 & 0 & 0 \\ 1 & 0 & 0 & 0 \\ 0 & 0 & 0 & -1 \\ 0 & 0 & -1 & 0 \end{pmatrix}, \\ O_{xy} &= J_x J_y + J_y J_x = i\sqrt{\frac{2}{3}}(-J_2^{(2)} + J_{-2}^{(2)}) \\ &= \sqrt{3} \begin{pmatrix} 0 & 0 & -i & 0 \\ 0 & 0 & 0 & -i \\ i & 0 & 0 & 0 \\ 0 & i & 0 & 0 \end{pmatrix}, \\ O_{yz} &= J_y J_z + J_z J_y = i\sqrt{\frac{2}{3}}(J_1^{(2)} + J_{-1}^{(2)}) \\ &= \sqrt{3} \begin{pmatrix} 0 & -i & 0 & 0 \\ i & 0 & 0 & 0 \\ 0 & 0 & 0 & i \\ 0 & 0 & -i & 0 \end{pmatrix}, \end{aligned} \quad (\text{A.3})$$

respectively. The Γ_4 octupole components are given by

$$\begin{aligned} T_x^\alpha &= \frac{1}{4}[\sqrt{5}(-J_3^{(3)} + J_{-3}^{(3)}) - \sqrt{3}(-J_1^{(3)} + J_{-1}^{(3)})] \\ &= \frac{3}{8} \begin{pmatrix} 0 & -\sqrt{3} & 0 & 5 \\ -\sqrt{3} & 0 & 3 & 0 \\ 0 & 3 & 0 & -\sqrt{3} \\ 5 & 0 & -\sqrt{3} & 0 \end{pmatrix}, \\ T_y^\alpha &= -\frac{i}{4}[\sqrt{5}(J_3^{(3)} + J_{-3}^{(3)}) + \sqrt{3}(J_1^{(3)} + J_{-1}^{(3)})] \\ &= \frac{3}{8} \begin{pmatrix} 0 & i\sqrt{3} & 0 & i5 \\ -i\sqrt{3} & 0 & -i3 & 0 \\ 0 & i3 & 0 & i\sqrt{3} \\ -i5 & 0 & -i\sqrt{3} & 0 \end{pmatrix}, \\ T_z^\alpha &= J_0^{(3)} \end{aligned}$$

$$= \frac{3}{4} \begin{pmatrix} 1 & 0 & 0 & 0 \\ 0 & -3 & 0 & 0 \\ 0 & 0 & 3 & 0 \\ 0 & 0 & 0 & -1 \end{pmatrix}. \quad (\text{A.4})$$

For Γ_5 ,

$$\begin{aligned} T_x^\beta &= -\frac{1}{4}[\sqrt{3}(-J_3^{(3)} + J_{-3}^{(3)}) + \sqrt{5}(-J_1^{(3)} + J_{-1}^{(3)})] \\ &= -\frac{3\sqrt{5}}{8} \begin{pmatrix} 0 & 1 & 0 & \sqrt{3} \\ 1 & 0 & -\sqrt{3} & 0 \\ 0 & -\sqrt{3} & 0 & 1 \\ \sqrt{3} & 0 & 1 & 0 \end{pmatrix}, \\ T_y^\beta &= \frac{i}{4}[-\sqrt{3}(J_3^{(3)} + J_{-3}^{(3)}) + \sqrt{5}(J_1^{(3)} + J_{-1}^{(3)})] \\ &= \frac{3\sqrt{5}}{8} \begin{pmatrix} 0 & -i & 0 & i\sqrt{3} \\ i & 0 & i\sqrt{3} & 0 \\ 0 & -i\sqrt{3} & 0 & -i \\ -i\sqrt{3} & 0 & i & 0 \end{pmatrix}, \\ T_z^\beta &= \frac{1}{\sqrt{2}}(J_2^{(3)} + J_{-2}^{(3)}) \\ &= \frac{3\sqrt{5}}{4} \begin{pmatrix} 0 & 0 & 1 & 0 \\ 0 & 0 & 0 & -1 \\ 1 & 0 & 0 & 0 \\ 0 & -1 & 0 & 0 \end{pmatrix}. \end{aligned} \quad (\text{A.5})$$

Lastly, the Γ_2 representation has a single component:

$$\begin{aligned} T_{xyz} &= \frac{i}{\sqrt{2}}(-J_2^{(3)} + J_{-2}^{(3)}) \\ &= \frac{3\sqrt{5}}{4} \begin{pmatrix} 0 & 0 & -i & 0 \\ 0 & 0 & 0 & i \\ i & 0 & 0 & 0 \\ 0 & -i & 0 & 0 \end{pmatrix}. \end{aligned} \quad (\text{A.6})$$

Appendix B: Unitary transformation for field direction as a quantization axis

The unitary transformation introduced in Sect 2.2 is expressed in the 4×4 form,

$$U = \begin{pmatrix} \chi^{-3}cc_{a+} & \chi^{-3}c\tilde{s} & \chi^{-3}s\tilde{s} & \chi^{-3}sc_{a-} \\ \chi^{-1}c\tilde{s} & \chi^{-1}cc_{b-} & -\chi^{-1}sc_{b+} & -\chi^{-1}s\tilde{s} \\ \chi s\tilde{s} & -\chi sc_{b+} & -\chi cc_{b-} & \chi c\tilde{s} \\ \chi^3sc_{a-} & -\chi^3s\tilde{s} & \chi^3c\tilde{s} & -\chi^3cc_{a+} \end{pmatrix}. \quad (\text{B.1})$$

Here, each matrix element comprises the following terms:

$$\begin{aligned} \chi &= e^{i\phi/2}, \quad c = \cos \frac{\theta}{2}, \quad s = \sin \frac{\theta}{2}, \quad \tilde{s} = \frac{\sqrt{3}}{2} \sin \theta, \\ c_{a\pm} &= \frac{1 \pm \cos \theta}{2}, \quad c_{b\pm} = \frac{1 \pm 3 \cos \theta}{2}. \end{aligned} \quad (\text{B.2})$$

The Zeeman term is anisotropic with respect to the field direction owing to the octupole components. For the transformed Zeeman term in Eq. (7), the coefficients f_i ($i = 1, 2, \dots, 7$) are listed as

$$\begin{aligned} f_1 &= \frac{B}{8} [(3 - 30 \cos^2 \theta + 35 \cos^4 \theta) + 5 \sin^4 \theta \cos 4\phi], \\ f_2 &= \frac{\sqrt{15}}{8} B \sin^2 \theta [(-1 + 7 \cos^2 \theta) + (1 + \cos^2 \theta) \cos 4\phi], \\ f_3 &= -\frac{\sqrt{15}}{4} B \sin^2 \theta \cos \theta \sin 4\phi, \end{aligned}$$

$$\begin{aligned}
 f_4 &= \frac{5\sqrt{6}}{16} B \sin \theta \cos \theta \left[(3 - 7 \cos^2 \theta) + \sin^2 \theta \cos 4\phi \right], \\
 f_5 &= \frac{\sqrt{10}}{16} B \sin \theta \cos \theta \left[7 \sin^2 \theta - (3 + \cos^2 \theta) \cos 4\phi \right], \\
 f_6 &= -\frac{5\sqrt{6}}{16} B \sin^3 \theta \sin 4\phi, \\
 f_7 &= \frac{\sqrt{10}}{16} B \sin \theta (1 + 3 \cos^2 \theta) \sin 4\phi. \tag{B.3}
 \end{aligned}$$

Appendix C: Unitary transformed quadrupole operators and strain-dependent coefficients

In Sect. 2.2, the unitary transformation has been introduced into the dipole and octupole terms in H_Z , as shown in Eqs. (6) and (7), respectively. For the quadrupole operators in Eq. (13), the unitary transformed O_k ($k = u, v, zx, xy, yz$) are written as

$$\begin{aligned}
 U^\dagger O_u U &= -\frac{1 - 3 \cos^2 \theta}{2} O_U + \frac{\sqrt{3}}{2} \sin^2 \theta O_V \\
 &\quad + \sqrt{3} \sin \theta \cos \theta O_{ZX}, \\
 U^\dagger O_v U &= \left(\frac{\sqrt{3}}{2} \sin^2 \theta O_U + \frac{1 + \cos^2 \theta}{2} O_V - \sin \theta \cos \theta O_{ZX} \right) \\
 &\quad \times \cos 2\phi \\
 &\quad + (-\cos \theta O_{XY} + \sin \theta O_{YZ}) \sin 2\phi, \\
 U^\dagger O_{zx} U &= (\sqrt{3} \sin \theta \cos \theta O_U - \sin \theta \cos \theta O_V - \cos 2\theta O_{ZX}) \\
 &\quad \times \cos \phi \\
 &\quad + (\sin \theta O_{XY} + \cos \theta O_{YZ}) \sin \phi, \\
 U^\dagger O_{xy} U &= \left(\frac{\sqrt{3}}{2} \sin^2 \theta O_U + \frac{1 + \cos^2 \theta}{2} O_V - \sin \theta \cos \theta O_{ZX} \right) \\
 &\quad \times \sin 2\phi \\
 &\quad + (\cos \theta O_{XY} - \sin \theta O_{YZ}) \cos 2\phi, \\
 U^\dagger O_{yz} U &= (\sqrt{3} \sin \theta \cos \theta O_U - \sin \theta \cos \theta O_V - \cos 2\theta O_{ZX}) \\
 &\quad \times \sin \phi \\
 &\quad + (-\sin \theta O_{XY} - \cos \theta O_{YZ}) \cos \phi. \tag{C.1}
 \end{aligned}$$

Accordingly, the strain-dependent coupling coefficients A_K have the following field-direction dependences:

$$\begin{aligned}
 A_U &= g_3 \left(-\varepsilon_u \frac{1 - 3 \cos^2 \theta}{2} + \frac{\sqrt{3}}{2} \varepsilon_v \sin^2 \theta \cos 2\phi \right) \\
 &\quad + g_5 \left[\frac{\sqrt{3}}{2} \varepsilon_{xy} \sin^2 \theta \sin 2\phi \right. \\
 &\quad \left. + \sqrt{3} \sin \theta \cos \theta (\varepsilon_{zx} \cos \phi + \varepsilon_{yz} \sin \phi) \right], \\
 A_V &= g_3 \left(\frac{\sqrt{3}}{2} \varepsilon_u \sin^2 \theta + \varepsilon_v \frac{1 + \cos^2 \theta}{2} \cos 2\phi \right) \\
 &\quad + g_5 \left[\varepsilon_{xy} \frac{1 + \cos^2 \theta}{2} \sin 2\phi - \sin \theta \cos \theta (\varepsilon_{zx} \cos \phi + \varepsilon_{yz} \sin \phi) \right], \\
 A_{ZX} &= g_3 \sin \theta \cos \theta (\sqrt{3} \varepsilon_u - \varepsilon_v \cos 2\phi) \\
 &\quad + g_5 \left[-\varepsilon_{xy} \sin \theta \cos \theta \sin 2\phi - \cos 2\theta (\varepsilon_{zx} \cos \phi + \varepsilon_{yz} \sin \phi) \right],
 \end{aligned}$$

$$\begin{aligned}
 A_{XY} &= -g_3 \varepsilon_v \cos \theta \sin 2\phi \\
 &\quad + g_5 \left[\varepsilon_{xy} \cos \theta \cos 2\phi + \sin \theta (\varepsilon_{zx} \sin \phi - \varepsilon_{yz} \cos \phi) \right], \\
 A_{YZ} &= g_3 \varepsilon_v \sin \theta \sin 2\phi \\
 &\quad + g_5 \left[-\varepsilon_{xy} \sin \theta \cos 2\phi + \cos \theta (\varepsilon_{zx} \sin \phi - \varepsilon_{yz} \cos \phi) \right]. \tag{C.2}
 \end{aligned}$$

Appendix D: Pseudospin-1/2 representation of the Γ_8 quartet and its relation to multipole operators for $J = 3/2$

Following Shiina *et al.*,³⁾ it is convenient to introduce two kinds of pseudospin-1/2 components representing spin (\uparrow, \downarrow) and orbital (\oplus, \ominus) degrees of freedom in the Γ_8 quartet. We connect the pseudospin representations to the multipole operators constructed from the $J = 3/2$ operators for the quartet. This is different from the way of using the original $J = 5/2$ operators in the earlier study.³⁾

First, the Γ_8 quartet is denoted by

$$\begin{aligned}
 |\Gamma_{8,1}\rangle &\rightarrow |3/2\rangle_{J_{\Gamma_8}=3/2} \rightarrow -|\oplus \downarrow\rangle, \\
 |\Gamma_{8,2}\rangle &\rightarrow |1/2\rangle_{J_{\Gamma_8}=3/2} \rightarrow |\ominus \uparrow\rangle, \\
 |\Gamma_{8,3}\rangle &\rightarrow |-1/2\rangle_{J_{\Gamma_8}=3/2} \rightarrow -|\ominus \downarrow\rangle, \\
 |\Gamma_{8,4}\rangle &\rightarrow |-3/2\rangle_{J_{\Gamma_8}=3/2} \rightarrow |\oplus \uparrow\rangle. \tag{D.1}
 \end{aligned}$$

The two components $\sigma (= \uparrow, \downarrow)$ are connected to each other by Pauli spin matrices $\sigma = (\sigma^x, \sigma^y, \sigma^z)$, and $\tau (= \oplus, \ominus)$ are connected by $\tau = (\tau^x, \tau^y, \tau^z)$ in the same manner. Each spin component and a product of two components τ^α and σ^β ($\alpha, \beta = x, y, z$) are related to the multipole operators constructed by $J = 3/2$ operators, which can be categorized by the irreducible representations of the O_h point group. For Γ_3 and Γ_5 quadrupole components,

$$\tau^z = \frac{1}{2\sqrt{3}} O_u, \quad \tau^x = \frac{1}{2\sqrt{3}} O_v, \tag{D.2}$$

and

$$2\tau^y \sigma^x = -\frac{1}{2\sqrt{3}} O_{yz}, \quad 2\tau^y \sigma^y = -\frac{1}{2\sqrt{3}} O_{zx}, \quad 2\tau^y \sigma^z = -\frac{1}{2\sqrt{3}} O_{xy}, \tag{D.3}$$

respectively. The linear combination of dipole and octupole components with the same representation Γ_4 are given by

$$\sigma^\mu = -\frac{1}{5} J_\mu - \frac{4}{15} T_\mu^\alpha \quad (\mu = x, y, z), \tag{D.4}$$

and

$$\begin{aligned}
 2\tau^z \sigma^z &= -\frac{2}{5} J_z + \frac{2}{15} T_z^\alpha, \\
 -\tau^z \sigma^x + \sqrt{3} \tau^x \sigma^x &= -\frac{2}{5} J_x + \frac{2}{15} T_x^\alpha, \\
 -\tau^z \sigma^y - \sqrt{3} \tau^y \sigma^y &= -\frac{2}{5} J_y + \frac{2}{15} T_y^\alpha. \tag{D.5}
 \end{aligned}$$

The other multipole components are Γ_5 and Γ_2 types written as

$$\begin{aligned}
 2\tau^x \sigma^z &= -\frac{2}{3\sqrt{5}} T_z^\beta, \\
 -\sqrt{3} \tau^z \sigma^x - \tau^x \sigma^x &= -\frac{2}{3\sqrt{5}} T_x^\beta,
 \end{aligned}$$

$$\sqrt{3}\tau^z\sigma^y - \tau^x\sigma^y = -\frac{2}{3\sqrt{5}}T_y^\beta, \quad (\text{D-6})$$

and

$$\tau^y = \frac{2}{3\sqrt{5}}T_{xyz}, \quad (\text{D-7})$$

respectively. As listed above, our representations are similar to those in Ref. 3 for the relationships between the $\tau \otimes \sigma$ representations and multipole components.

Appendix E: Multipole–multipole interaction model

The spherical multipole–multipole interaction is invariant under the rotation of a magnetic field. On the other hand, the Zeeman splitting is anisotropic for the Γ_8 quartet in Eq. (D-1) owing to the different octupole components in the Zeeman term, as shown in Eq. (31). This is a crucial point for the multipole symmetry of an induced ordered moment depending on the field direction.

The highly spherical interaction is given by the following Hamiltonian:^{3,46,47)}

$$H_S = D \sum_{\langle i,j \rangle} [\boldsymbol{\sigma}_i \cdot \boldsymbol{\sigma}_j + \boldsymbol{\tau}_i \cdot \boldsymbol{\tau}_j + 4(\boldsymbol{\tau}_i \cdot \boldsymbol{\tau}_j)(\boldsymbol{\sigma}_i \cdot \boldsymbol{\sigma}_j)] + H_Z. \quad (\text{E-1})$$

Here, the first term consists of spin, orbital, and spin + orbital interactions between the nearest-neighbor i and j sites with coupling constant D (> 0). This interaction is SU(4) symmetric with respect to the 4×4 pseudospin space $\tau \otimes \sigma$. The last term H_Z represents the Zeeman splitting of the quartet denoted by $|\tau, \sigma\rangle$,

$$H_Z = \sum_i \left[(1 + 3\lambda)\boldsymbol{\sigma}_i + \frac{4 - 3\lambda}{2}\boldsymbol{\eta}_i \right] \cdot \mathbf{B} \quad (B = g\mu_B H), \quad (\text{E-2})$$

where the vectorial octupole operator $\boldsymbol{\eta}$ is given by the product of $\boldsymbol{\tau}$ and $\boldsymbol{\sigma}$ components:³⁾

$$(\eta^x, \eta^y, \eta^z) = (-\tau^z\sigma^x + \sqrt{3}\tau^x\sigma^x, -\tau^z\sigma^y - \sqrt{3}\tau^x\sigma^y, 2\tau^z\sigma^z). \quad (\text{E-3})$$

These components correspond to those in Eq. (D-5). Indeed, the highly symmetric interaction terms can be divided into nonmagnetic and magnetic sectors as $H_S = H_Q + H_M + H_Z$:

$$\begin{aligned} H_Q &= D_Q \sum_{\langle i,j \rangle} [(\tilde{\tau}_i^z \tilde{\tau}_j^z + \tilde{\tau}_i^x \tilde{\tau}_j^x) + (\tilde{\tau}_i^y \tilde{\sigma}_i) \cdot (\tilde{\tau}_j^y \tilde{\sigma}_j)] \\ &= \frac{D_Q}{3} \sum_{\langle i,j \rangle} \sum_{\mu} O_{i,\mu} O_{j,\mu} \quad (\mu = u, v, yz, zx, xy), \end{aligned} \quad (\text{E-4})$$

$$\begin{aligned} H_M &= D_M \sum_{\langle i,j \rangle} [\tilde{\sigma}_i \cdot \tilde{\sigma}_j + (\tilde{\tau}_i^z \tilde{\sigma}_i) \cdot (\tilde{\tau}_j^z \tilde{\sigma}_j) + (\tilde{\tau}_i^x \tilde{\sigma}_i) \cdot (\tilde{\tau}_j^x \tilde{\sigma}_j) + \tilde{\tau}_i^y \tilde{\tau}_j^y] \\ &= \frac{4}{5} D_M \left\{ \sum_{\mu=x,y,z} J_{i,\mu} J_{j,\mu} + \frac{4}{9} \left[\sum_{\mu=x,y,z} (T_{i,\mu}^\alpha T_{j,\mu}^\alpha + T_{i,\mu}^\beta T_{j,\mu}^\beta) \right. \right. \\ &\quad \left. \left. + T_{i,xyz} T_{j,xyz} \right] \right\}, \end{aligned} \quad (\text{E-5})$$

where $\tilde{\sigma} = 2\sigma$ and $\tilde{\tau} = 2\tau$. The coupling constants satisfy $D_Q = D_M = D$ for the SU(4) symmetric model.

Appendix F: Transition temperatures for the three typical axes of a low magnetic field

Here, we discuss the octupole effects on the antiferroquadrupole order phase using the GL expansion of the free energy for the spherical multipole–multipole interaction model in Sect. 3.3. The anisotropy arising from the octupoles is represented by the parameter λ in Eq. (5). For a deeper understanding of the octupole effects, it is very useful to compare the GL expansion for both $\mathbf{H} \parallel [111]$ and $\mathbf{H} \parallel [110]$ with that for $\mathbf{H} \parallel [001]$ studied by Shiina *et al.*³⁾

F.1 $\mathbf{H} \parallel [001]$ case

The low-field antiferroquadrupole O_u (τ^Z) phase is described by the relevant staggered quadrupole moment $\tilde{\tau}_{\text{af}}^Z$, other staggered moments ($\tilde{\sigma}_{\text{af}}^Z, \tilde{\eta}_{\text{af}}^Z$), and uniform moments ($\tilde{\tau}_f^Z, \tilde{\sigma}_f^Z, \tilde{\eta}_f^Z$) induced by the quadrupole order under the applied magnetic field. The GL free energy is expanded up to the third order in which three kinds of multipoles (dipole, quadrupole, and octupole) are coupled to each other. With the increase in the field strength, the quadrupole order is stabilized by the third order of the free energy given by

$$F_{[001]}^{(3)} = -T(\tilde{\tau}_{\text{af}}^Z \tilde{\sigma}_f^Z \tilde{\eta}_{\text{af}}^Z + \tilde{\eta}_{\text{af}}^Z \tilde{\tau}_f^Z \tilde{\sigma}_{\text{af}}^Z + \tilde{\sigma}_{\text{af}}^Z \tilde{\eta}_f^Z \tilde{\tau}_{\text{af}}^Z + \tilde{\tau}_f^Z \tilde{\sigma}_f^Z \tilde{\eta}_f^Z). \quad (\text{F-1})$$

Combining $F^{(3)}$ with the second-order and Zeeman terms, we represent the free energy as

$$\begin{aligned} F - F_0 &= \frac{1}{2}(T - T_0^Q)(\tilde{\tau}_{\text{af}}^Z)^2 + \frac{1}{2}(T - T_0^M) \sum_{\gamma=\sigma,\eta} (\tilde{\gamma}_{\text{af}}^Z)^2 \\ &\quad + \frac{1}{2}(T + T_0^Q)(\tilde{\tau}_f^Z)^2 + \frac{1}{2}(T + T_0^M) \sum_{\gamma=\sigma,\eta} (\tilde{\gamma}_f^Z)^2 \\ &\quad + F_{[001]}^{(3)} - B \left(\frac{1 + 3\lambda}{2} \tilde{\sigma}_f^Z + \frac{4 - 3\lambda}{4} \tilde{\eta}_f^Z \right) - \delta h_s \tilde{\tau}_{\text{af}}^Z, \end{aligned} \quad (\text{F-2})$$

where F_0 is the origin of the free energy for the paraquadrupole phase, and $T_0^Q \gtrsim T_0^M$ is assumed for the transition temperatures at the zero field. δh_s is a fictitious staggered field related to the transition temperature at a finite field B .³⁾ Minimizing the free energy with respect to $\tilde{\tau}_{\text{af}}^Z$, $\tilde{\sigma}_{\text{af}}^Z$, and $\tilde{\eta}_{\text{af}}^Z$, we leave the leading terms to determine the transition temperature,

$$\left\{ T - T_0^Q - \frac{T^2 [(\tilde{\sigma}_f^Z)^2 + (\tilde{\eta}_f^Z)^2]}{T - T_0^M} \right\} \tilde{\tau}_{\text{af}}^Z = \delta h_s. \quad (\text{F-3})$$

For a finite B , the free energy is minimized with respect to $\tilde{\sigma}_f$ and $\tilde{\eta}_f$, which leads to the Curie–Weiss law:

$$\tilde{\sigma}_f^Z = \frac{1 + 3\lambda}{2} \frac{B}{T + T_0^M}, \quad \tilde{\eta}_f^Z = \frac{4 - 3\lambda}{4} \frac{B}{T + T_0^M}. \quad (\text{F-4})$$

The transition temperature at a finite field is given by the solution for $\delta h_s \rightarrow 0$. After substituting $\tilde{\sigma}_f$ and $\tilde{\eta}_f$ in Eq. (F-3), we obtain the leading contribution of B to the transition temperature:

$$T^Q = T_0^Q + \frac{5(4 + 9\lambda^2)}{64} \frac{B^2}{T_0^Q - T_0^M}. \quad (\text{F-5})$$

This indicates that the increase in T^Q is proportional to B^2 ($B = g\mu_B H$) and its proportionality coefficient is increased

by the octupole effect with λ . In the symmetric limit $T_0^M \rightarrow T_0^Q$, the transition temperature shows a linear B dependence

$$T^Q = T_0^Q + \frac{\sqrt{5(4+9\lambda^2)}}{8} B. \quad (\text{F.6})$$

F.2 $\mathbf{H} \parallel [111]$ case

The above argument for $\mathbf{H} \parallel [001]$ can be applied to the antiferroquadrupole $O_{yz} + O_{zx} + O_{xy}$ phase denoted by τ^Z for $\mathbf{H} \parallel [111]$ straightforwardly. The only difference is that the Zeeman term in Eq. (31) includes the effective transverse component $(\tilde{\sigma}^X + \tilde{\eta}^X)B$ other than $\tilde{\sigma}^Z B$ and $\tilde{\eta}^Z B$, which leads to the coupling of $|3/2\rangle$ and $|-3/2\rangle$, as shown in Table I. Accordingly, the additional moments $\tilde{\sigma}_f^X$, $\tilde{\eta}_f^X$, $\tilde{\sigma}_{\text{af}}^X$, and $\tilde{\eta}_{\text{af}}^X$ are induced together with $\tilde{\sigma}_f^Z$, $\tilde{\eta}_f^Z$, $\tilde{\sigma}_{\text{af}}^Z$, and $\tilde{\eta}_{\text{af}}^Z$ simultaneously. The Zeeman term can be rewritten as

$$\begin{aligned} H_{Z,[111]} &= -B \left[\frac{1-2\lambda}{2} \tilde{\sigma}_f^Z + \frac{2+\lambda}{2} \tilde{\eta}_f^Z + \frac{5\lambda}{4\sqrt{2}} (\tilde{\sigma}_f^X + \tilde{\eta}_f^X) \right] \\ &= -B \left(\frac{G_\lambda}{4} \tilde{\xi}_f^+ + \frac{1+3\lambda}{2} \tilde{\xi}_f^- \right), \end{aligned} \quad (\text{F.7})$$

where G_λ is given in Table I. The new parameters $\tilde{\xi}_{\text{f(af)}}^\pm$ of uniform (staggered) moments are related to the above eight moments as

$$\begin{aligned} \tilde{\sigma}_{\text{f(af)}}^Z &= \tilde{\xi}_{\text{f(af)}}^+ \cos 2\theta_d - \tilde{\xi}_{\text{f(af)}}^-, \\ \tilde{\eta}_{\text{f(af)}}^Z &= \tilde{\xi}_{\text{f(af)}}^+ \cos 2\theta_d + \tilde{\xi}_{\text{f(af)}}^-, \\ \tilde{\sigma}_{\text{f(af)}}^X &= \tilde{\eta}_{\text{f(af)}}^X = \tilde{\xi}_{\text{f(af)}}^+ \sin 2\theta_d, \\ (\cos 2\theta_d &= d_+^2 - d_-^2, \quad \sin 2\theta_d = 2d_+ d_-). \end{aligned} \quad (\text{F.8})$$

Using $\tilde{\xi}^\pm$ instead of $\tilde{\sigma}^Z$, $\tilde{\eta}^Z$, $\tilde{\sigma}^X$ and $\tilde{\eta}^X$, the GL free energy is expanded to the third order,

$$\begin{aligned} F - F_0 &= \frac{1}{2} (T - T_0^Q) (\tilde{\tau}_{\text{af}}^Z)^2 + (T - T_0^M) \sum_{\mu=+,-} (\tilde{\xi}_{\text{af}}^\mu)^2 \\ &+ \frac{1}{2} (T + T_0^Q) (\tilde{\tau}_f^Z)^2 + (T + T_0^M) \sum_{\mu=+,-} (\tilde{\xi}_f^\mu)^2 \\ &+ F_{[111]}^{(3)} + H_{Z,[111]} - \delta h_s \tilde{\tau}_{\text{af}}^Z, \end{aligned} \quad (\text{F.9})$$

and

$$\begin{aligned} F_{[111]}^{(3)} &= -T (\tilde{\tau}_{\text{af}}^Z \tilde{\sigma}_f^Z \tilde{\eta}_{\text{af}}^Z + \tilde{\tau}_{\text{af}}^Z \tilde{\sigma}_f^X \tilde{\eta}_{\text{af}}^X + \tilde{\eta}_{\text{af}}^Z \tilde{\tau}_f^Z \tilde{\sigma}_{\text{af}}^Z + \tilde{\eta}_{\text{af}}^X \tilde{\tau}_f^X \tilde{\sigma}_{\text{af}}^X \\ &+ \tilde{\sigma}_{\text{af}}^Z \tilde{\eta}_f^Z \tilde{\tau}_{\text{af}}^Z + \tilde{\sigma}_{\text{af}}^X \tilde{\eta}_f^X \tilde{\tau}_{\text{af}}^X + \tilde{\tau}_f^Z \tilde{\sigma}_f^Z \tilde{\eta}_f^Z + \tilde{\tau}_f^X \tilde{\sigma}_f^X \tilde{\eta}_f^X) \\ &= -T \left\{ 2\tilde{\tau}_{\text{af}}^Z (\tilde{\xi}_f^+ \tilde{\xi}_{\text{af}}^+ - \tilde{\xi}_f^- \tilde{\xi}_{\text{af}}^-) \right. \\ &\left. + \tilde{\tau}_f^+ \left[(\tilde{\xi}_{\text{af}}^+)^2 - (\tilde{\xi}_{\text{af}}^-)^2 + (\tilde{\xi}_f^+)^2 - (\tilde{\xi}_f^-)^2 \right] \right\}. \end{aligned} \quad (\text{F.10})$$

Minimizing the free energy with respect to $\tilde{\tau}_{\text{af}}^Z$, $\tilde{\xi}_{\text{af}}^+$, and $\tilde{\xi}_{\text{af}}^-$ at $\delta h_s \rightarrow 0$, we obtain the transition temperature increased by the applied field as

$$T^Q = T_0^Q + \frac{2(T_0^Q)^2}{T_0^Q - T_0^M} \sum_{\mu=+,-} (\tilde{\xi}_f^\mu)^2. \quad (\text{F.11})$$

On the other hand, the Curie–Weiss law is represented by

$$\tilde{\xi}_f^+ = \frac{G_\lambda}{8} \frac{B}{T + T_0^M}, \quad \tilde{\xi}_f^- = \frac{1+3\lambda}{4} \frac{B}{T + T_0^M}. \quad (\text{F.12})$$

Finally, T^Q for $T_0^Q \gtrsim T_0^M$ is obtained as

$$T^Q = T_0^Q + \frac{5(4+9\lambda^2)}{64} \frac{B^2}{T_0^Q - T_0^M}. \quad (\text{F.13})$$

Note that this is the same as T^Q for $\mathbf{H} \parallel [001]$.³⁾

F.3 $\mathbf{H} \parallel [110]$ case

For $\mathbf{H} \parallel [110]$, the Zeeman term includes $\tilde{\tau}^Z B = \tilde{\tau}^X \tilde{\sigma}^Z B$, which leads to the coupling of $|3/2\rangle$ and $|-1/2\rangle$ and that of $|1/2\rangle$ and $|-3/2\rangle$. As a consequence, the magnetic field can also induce the uniform and staggered quadrupole moments denoted by τ^X . Introducing a new parameter $\tilde{\xi}_{\text{f(af)}}^Z$ related to the uniform (staggered) moments $\tilde{\eta}_{\text{f(af)}}^Z$ and $\tilde{\xi}_{\text{f(af)}}^Z$ as

$$\begin{aligned} \tilde{\eta}_{\text{f(af)}}^Z &= \tilde{\xi}_{\text{f(af)}}^Z \cos 2\theta_c, \quad \tilde{\xi}_{\text{f(af)}}^Z = -\tilde{\xi}_{\text{f(af)}}^Z \sin 2\theta_c, \\ (\cos 2\theta_c &= c_+^2 - c_-^2, \quad \sin 2\theta_c = 2c_+ c_-), \end{aligned} \quad (\text{F.14})$$

we can rewrite the Zeeman term as

$$\begin{aligned} H_{Z,[110]} &= -\frac{B}{16} \left[(8-6\lambda) \tilde{\sigma}_f^Z + (16+3\lambda) \tilde{\eta}_f^Z - 15\sqrt{3}\lambda \tilde{\xi}_f^Z \right] \\ &= -B \left(\frac{4-3\lambda}{8} \tilde{\sigma}_f^Z + \frac{F_\lambda}{16} \tilde{\xi}_f^Z \right), \end{aligned} \quad (\text{F.15})$$

where F_λ is given in Table I. In addition, we represent primary order parameters $\tau_{\text{f(af)}}^Z$ and $\tau_{\text{f(af)}}^X$ by the linear combination of new parameters τ' and τ'' as

$$\begin{aligned} \tau_{\text{f(af)}}^Z &= \tau'_{\text{f(af)}} \cos 2\theta_c - \tau''_{\text{f(af)}} \sin 2\theta_c, \\ \tau_{\text{f(af)}}^X &= -\tau'_{\text{f(af)}} \sin 2\theta_c - \tau''_{\text{f(af)}} \cos 2\theta_c. \end{aligned} \quad (\text{F.16})$$

For the expansion of the GL energy up to the third order, the leading terms are obtained as

$$\begin{aligned} F - F_0 &= \frac{1}{2} (T - T_0^Q) (\tilde{\tau}_{\text{af}}^Z)^2 + \frac{1}{2} (T - T_0^M) \sum_{\gamma=\sigma^Z, \xi} \tilde{\gamma}_{\text{af}}^2 \\ &+ \frac{1}{2} (T + T_0^Q) (\tilde{\tau}_f^Z)^2 + \frac{1}{2} (T + T_0^M) \sum_{\gamma=\sigma^Z, \xi} \tilde{\gamma}_f^2 \\ &+ F_{[110]}^{(3)} + H_{Z,[110]} - \delta h_s \tilde{\tau}_{\text{af}}^Z, \end{aligned} \quad (\text{F.17})$$

and

$$\begin{aligned} F_{[110]}^{(3)} &= -T (\tilde{\tau}_{\text{af}}^Z \tilde{\sigma}_f^Z \tilde{\eta}_{\text{af}}^Z + \tilde{\tau}_{\text{af}}^X \tilde{\sigma}_f^Z \tilde{\xi}_{\text{af}}^Z + \tilde{\eta}_{\text{af}}^Z \tilde{\tau}_f^Z \tilde{\sigma}_{\text{af}}^Z + \tilde{\xi}_{\text{af}}^Z \tilde{\tau}_f^X \tilde{\sigma}_{\text{af}}^Z \\ &+ \tilde{\sigma}_{\text{af}}^Z \tilde{\eta}_f^Z \tilde{\tau}_{\text{af}}^Z + \tilde{\sigma}_{\text{af}}^X \tilde{\eta}_f^Z \tilde{\tau}_{\text{af}}^X + \tilde{\tau}_f^Z \tilde{\sigma}_f^Z \tilde{\eta}_f^Z + \tilde{\tau}_f^X \tilde{\sigma}_f^Z \tilde{\xi}_f^Z) \\ &= -T (\tilde{\tau}_{\text{af}}^Z \tilde{\sigma}_f^Z \tilde{\xi}_{\text{af}}^Z + \tilde{\xi}_{\text{af}}^Z \tilde{\tau}_f^Z \tilde{\sigma}_{\text{af}}^Z + \tilde{\sigma}_{\text{af}}^Z \tilde{\xi}_f^Z \tilde{\tau}_{\text{af}}^Z + \tilde{\tau}_f^Z \tilde{\sigma}_f^Z \tilde{\xi}_f^Z). \end{aligned} \quad (\text{F.18})$$

We note that the form of Eq. (F.17) is similar to that of Eq. (F.2). Thus, the transition temperature for $T_0^Q \gtrsim T_0^M$ is calculated up to the order of B^2 as

$$\begin{aligned} T^Q &= T_0^Q + \frac{B^2}{4(T_0^Q - T_0^M)} \left[\left(\frac{4-3\lambda}{8} \right)^2 + \left(\frac{F_\lambda}{16} \right)^2 \right] \\ &= T_0^Q + \frac{5(4+9\lambda^2)}{64} \frac{B^2}{T_0^Q - T_0^M}. \end{aligned} \quad (\text{F.19})$$

The result is that the increase in T^Q for $\mathbf{H} \parallel [110]$ shows the same field dependence as that for $\mathbf{H} \parallel [001]$ and $[111]$.³⁾ The stabilized quadrupole component is written as

$$\tilde{\tau}^Z = \tilde{\tau}^Z \cos 2\theta_c - \tilde{\tau}^X \sin 2\theta_c$$

$$= \frac{1}{\sqrt{3}F_\lambda} [(16 + 3\lambda)O_U - 15\sqrt{3}\lambda \cdot O_V], \quad (\text{F}\cdot 20)$$

and it has only diagonal matrix elements for the eigenstates in Table I: $\langle \psi_{1(4)} | \tilde{\tau}' | \psi_{1(4)} \rangle = 1$ and $\langle \psi_{2(3)} | \tilde{\tau}' | \psi_{2(3)} \rangle = -1$ for $\mathbf{H} \parallel [110]$. Using the unitary transformation in Eq. (C·1), the two components O_U and O_V of $\tilde{\tau}'$ are represented by the linear combination of O_u and O_{xy} in the original (xyz) reference frame as

$$O_U \rightarrow -\frac{1}{2}O_u + \frac{\sqrt{3}}{2}O_{xy}, \quad O_V \rightarrow \frac{\sqrt{3}}{2}O_u + \frac{1}{2}O_{xy} \quad (\text{F}\cdot 21)$$

for the SU(4) symmetric interaction model.

-
- 1) P. Santini, S. Carretta, G. Amoretti, R. Caciuffo, N. Magnani, and G. H. Lander, *Rev. Mod. Phys.* **81**, 807 (2009).
 - 2) Y. Kuramoto, H. Kusunose, and A. Kiss, *J. Phys. Soc. Jpn.* **78**, 072001 (2009).
 - 3) R. Shiina, H. Shiba, and P. Thalmeier, *J. Phys. Soc. Jpn.* **66**, 1741 (1997).
 - 4) A. Hernández-Mínguez, A. V. Poshakinskiy, M. Hollenbach, P. V. Santos, and G. V. Astakhov, *Sci. Adv.* **7**, eabj5030 (2021).
 - 5) T. Vasselon, A. Hernández-Mínguez, M. Hollenbach, G. V. Astakhov, and P. V. Santos, *Phys. Rev. Appl.* **20**, 034017 (2023).
 - 6) J. R. Dietz, B. Jiang, A. M. Day, S. A. Bhave, and E. L. Hu, *Nat. Electron.* **6**, 739 (2023).
 - 7) A. Hernández-Mínguez, A. V. Poshakinskiy, M. Hollenbach, P. V. Santos, and G. V. Astakhov, *Phys. Rev. Lett.* **125**, 107702 (2020).
 - 8) M. Koga and M. Matsumoto, *J. Phys. Soc. Jpn.* **93**, 014703 (2024).
 - 9) V. A. Soltamov, C. Kasper, A. V. Poshakinskiy, A. N. Anisimov, E. N. Mokhov, A. Sperlich, S. A. Tarasenko, P. G. Baranov, G. V. Astakhov, and V. Dyakonov, *Nat. Commun.* **10**, 1678 (2019).
 - 10) H. Kraus, V. A. Soltamov, D. Riedel, S. Váth, F. Fuchs, A. Sperlich, P. G. Baranov, V. Dyakonov, and G. V. Astakhov, *Nat. Phys.* **10**, 157 (2014).
 - 11) M. Widmann, S.-Y. Lee, T. Rendler, N. T. Son, H. Fedder, S. Paik, L.-P. Yang, N. Zhao, S. Yang, I. Booker, A. Denisenko, M. Jamali, S. A. Momenzadeh, I. Gerhardt, T. Ohshima, A. Gali, E. Jánzén, and J. Wrachtrup, *Nat. Mater.* **14**, 164 (2015).
 - 12) D. Simin, H. Kraus, A. Sperlich, T. Ohshima, G. V. Astakhov, and V. Dyakonov, *Phys. Rev. B* **95**, 161201(R) (2017).
 - 13) R. Nagy, M. Widmann, M. Niethammer, D. B. R. Dasari, I. Gerhardt, Ö. O. Soykal, M. Radulaski, T. Ohshima, J. Vučković, N. T. Son, I. G. Ivanov, S. E. Economou, C. Bonato, S.-Y. Lee, and J. Wrachtrup, *Phys. Rev. Appl.* **9**, 034022 (2018).
 - 14) S. Castelletto and A. Boretti, *J. Phys.: Photonics* **2**, 022001 (2020).
 - 15) N. T. Son, C. P. Anderson, A. Bourassa, K. C. Miao, C. Babin, M. Widmann, M. Niethammer, J. U. Hassan, N. Morioka, I. G. Ivanov, F. Kaiser, J. Wrachtrup, and D. D. Awschalom, *Appl. Phys. Lett.* **116**, 190501 (2020).
 - 16) O. Sakai, R. Shiina, H. Shiba, and P. Thalmeier, *J. Phys. Soc. Jpn.* **66**, 3005 (1997).
 - 17) R. Shiina, O. Sakai, H. Shiba, and P. Thalmeier, *J. Phys. Soc. Jpn.* **67**, 941 (1998).
 - 18) H. Shiba, O. Sakai, and R. Shiina, *J. Phys. Soc. Jpn.* **68**, 1988 (1999).
 - 19) D. Mannix, Y. Tanaka, D. Carbone, N. Bernhoeft, and S. Kunii, *Phys. Rev. Lett.* **95**, 117206 (2005).
 - 20) H. Kusunose and Y. Kuramoto, *J. Phys. Soc. Jpn.* **74**, 3139 (2005).
 - 21) T. Nagao and J. Igarashi, *Phys. Rev. B* **74**, 104404 (2006).
 - 22) T. Matsumura, T. Yonemura, K. Kunimori, M. Sera, and F. Iga, *Phys. Rev. Lett.* **103**, 017203 (2009).
 - 23) T. Nagao and J. Igarashi, *Phys. Rev. B* **82**, 024402 (2010).
 - 24) T. Matsumura, T. Yonemura, K. Kunimori, M. Sera, F. Iga, T. Nagao, and J. Igarashi, *Phys. Rev. B* **85**, 174417 (2012).
 - 25) P. Y. Portnichenko, A. Akbari, S. E. Nikitin, A. S. Cameron, A. V. Dukhnenko, V. B. Filipov, N. Yu. Shitsevalova, P. Čermák, I. Radelytskyi, A. Schneidewind, J. Ollivier, A. Podlesnyak, Z. Huesges, J. Xu, A. Ivanov, Y. Sidis, S. Petit, J.-M. Mignot, P. Thalmeier, and D. S. Inosov, *Phys. Rev. X* **10**, 021010 (2020).
 - 26) M. Koga and M. Matsumoto, *J. Phys. Soc. Jpn.* **89**, 024701 (2020).
 - 27) M. Matsumoto and M. Koga, *J. Phys. Soc. Jpn.* **89**, 084702 (2020).
 - 28) M. Koga and M. Matsumoto, *J. Phys. Soc. Jpn.* **89**, 113701 (2020).
 - 29) M. Koga and M. Matsumoto, *J. Phys. Soc. Jpn.* **91**, 094709 (2022).
 - 30) I. Gromov and A. Schweiger, *J. Magn. Reson.* **146**, 110 (2000).
 - 31) M. Kälin, I. Gromov, and A. Schweiger, *Phys. Rev. A* **69**, 033809 (2004).
 - 32) Z. György, A. Pályi, and G. Széchenyi, *Phys. Rev. B* **106**, 155412 (2022).
 - 33) J. H. Shirley, *Phys. Rev.* **138**, B979 (1965).
 - 34) S.-K. Son, S. Han, and S. I. Chu, *Phys. Rev. A* **79**, 032301 (2009).
 - 35) T. Inui, Y. Tanabe, and Y. Onodera, *Group Theory and Its Applications in Physics* (Springer, Berlin, 1990).
 - 36) S. Nakamura, T. Goto, S. Kunii, K. Iwashita, and A. Tamaki, *J. Phys. Soc. Jpn.* **63**, 623 (1994).
 - 37) M. Takigawa, H. Yasuoka, T. Tanaka, and Y. Ishizawa, *J. Phys. Soc. Jpn.* **52**, 728 (1983).
 - 38) A. V. Semeno, M. I. Gilmanov, A. V. Bogach, V. N. Krasnorussky, A. N. Samarin, N. A. Samarin, N. E. Sluchanko, N. Yu. Shitsevalova, V. B. Filipov, V. V. Glushkov, and S. V. Demishev, *Sci. Rep.* **6**, 39196 (2016).
 - 39) P. Schlottmann, *Magnetochemistry* **4**, 27 (2018).
 - 40) A. V. Semeno, S. Okubo, H. Ohta, and S. V. Demishev, *Appl. Magn. Reson.* **52**, 459 (2021).
 - 41) T. Mito, H. Mori, K. Miyamoto, T. Tanaka, Y. Nakai, K. Ueda, F. Iga, and H. Harima, *J. Phys. Soc. Jpn.* **92**, 034702 (2023).
 - 42) D. Simin, V. A. Soltamov, A. V. Poshakinskiy, A. N. Anisimov, R. A. Babunts, D. O. Tolmachev, E. N. Mokhov, M. Trupke, S. A. Tarasenko, A. Sperlich, P. G. Baranov, V. Dyakonov, and G. V. Astakhov, *Phys. Rev. X* **6**, 031014 (2016).
 - 43) S. A. Tarasenko, A. V. Poshakinskiy, D. Simin, V. A. Soltamov, E. N. Mokhov, P. G. Baranov, V. Dyakonov, and G. V. Astakhov, *Phys. Status Solidi B* **255**, 1700258 (2018).
 - 44) P. Udvarhelyi, V. O. Shkolnikov, A. Gali, G. Burkard, and A. Pályi, *Phys. Rev. B* **98**, 075201 (2018).
 - 45) P. Udvarhelyi and A. Gali, *Phys. Rev. Appl.* **10**, 054010 (2018).
 - 46) F. J. Ohkawa, *J. Phys. Soc. Jpn.* **52**, 3897 (1983).
 - 47) F. J. Ohkawa, *J. Phys. Soc. Jpn.* **54**, 3909 (1985).